PHYSICAL REVIEW B **96**, 020405(R) (2017)

Multiscale simulations of topological transformations in magnetic-skyrmion spin structures

Andrea De Lucia,[1,2] Kai Litzius,[1,2,3] Benjamin Krüger,[1] Oleg A. Tretiakov,[4,5] and Mathias Kläui[1,2]

[1]*Institute of Physics, Johannes Gutenberg University Mainz, Staudingerweg 7, 55128 Mainz, Germany*

[2]*Graduate School of Excellence - Materials Science in Mainz, Staudingerweg 9, 55128 Mainz, Germany*

[3]*Max Planck Institute for Intelligent Systems, Heisenbergstrasse 1, 70569 Stuttgart, Germany*

[4]*Institute for Materials Research, Tohoku University, Sendai 980-8577, Japan*

[5]*School of Natural Sciences, Far Eastern Federal University, Vladivostok 690950, Russia*

(Received 1 March 2017; published 11 July 2017)

Magnetic skyrmions belong to the most interesting spin structures for the development of future information technology as they have been predicted to be topologically protected. To quantify their stability, we use an innovative multiscale approach to simulating spin dynamics based on the Landau-Lifshitz-Gilbert equation. The multiscale approach overcomes the micromagnetic limitations that have hindered realistic studies using conventional techniques. We first demonstrate how the stability of a skyrmion is influenced by the refinement of the computational mesh and reveal that conventionally employed traditional micromagnetic simulations are inadequate for this task. Furthermore, we determine the stability quantitatively using our multiscale approach. As a key operation for devices, the process of annihilating a skyrmion by exciting it with a spin polarized current pulse is analyzed, showing that skyrmions can be reliably deleted by designing the pulse shape.

DOI: 10.1103/PhysRevB.96.020405

I. INTRODUCTION

Magnetic skyrmions [1] are topological spin structures that arise in the spin pattern of ferromagnetic systems with broken inversion symmetry, such as chiral crystals [2,3] or thin chiral magnetic films [4,5]. Skyrmion lattices [6–9] constitute the ground state for some systems, while isolated skyrmions can appear as metastable states of some magnetic nanostructures [10]. Isolated skyrmions have been recently considered [11–15] as the building blocks for ultradense magnetic storage devices [16].

Skyrmions carry a topological charge $Q = \pm 1$ defined as [17]:

$$Q = \int_A q\, dxdy = \frac{1}{4\pi}\int_A \mathbf{m}\cdot\left(\frac{\partial \mathbf{m}}{\partial x}\times\frac{\partial \mathbf{m}}{\partial y}\right)dxdy, \quad (1)$$

where q is the topological charge density, A the area of the system, and $\mathbf{m}$ the unit magnetization vector. Since transitions that change Q are forbidden [17] in a continuum description of $\mathbf{m}$, such structures are topologically protected. Nevertheless, in a real system composed of discrete magnetic moments localized on the atomic lattice sites, no strict topological protection exists [18]. Thus it is necessary to overcome a finite energy barrier to induce transformations that change Q [17,19–21], such as the annihilation of a Bloch line (BL) [21–26]. Since it maximizes locally the exchange energy, the BL formation process likely includes an energy saddle point.

The stability against perturbations is indeed a key feature of skyrmions, making them a good candidate as information carriers in next generation storage devices [27–29]. The fundamental prerequisites for applications are ascertaining the stability of skyrmions, as well as reliably annihilating them. However, the computational treatment of processes involving annihilating skyrmions is very delicate. In analytical micromagnetic theory, singularities in the exchange field tend to arise during topological transformations, making numerical simulations very susceptible to the mesh being used [30] and therefore often inaccurate. The necessity for a computational model, capable of performing quantitatively accurate simulations is therefore obvious and a key step. While more accurate atomistic simulations would overcome this problem, the computational power required to run such simulations for a sample of realistic experimental size makes this possibility not feasible.

In this Rapid Communication, the annihilation of isolated skyrmions is studied by simulating the Landau-Lifshitz-Gilbert (LLG) equation with a multiscale approach at 0 K [31]. Within this approach the core of the skyrmion is simulated atomistically, while the remaining part of a nanodisk hosting the skyrmion is simulated using micromagnetics. This technique was designed to ensure computational accuracy combined with feasible computational times. Though multiscale simulations are a well established method in computational micromagnetism [32–41], the research presented here constitutes the first application of an approach capable of selectively employing different models to different regions of the magnetic system according to the peculiarities of the magnetization structure of interest. A quantitative demonstration of the limitations of the micromagnetic model and a brief description of the multiscale approach [31] are given in the Supplemental Material [42].

First, the effects of the lattice on the stability are studied, showing how the mesh density influences the annihilation of skyrmions. Then, BLs are excited along the domain wall separating the two out-of-plane magnetized domains in the skyrmion. For this purpose we employ current pulses that generate spin-orbit torques [43–45], showing how the shape of these pulses influences the skyrmion and induces changes to the topology. The application of spin-orbit torques to skyrmions constitutes a topical field of research. While analytical continuum theory cannot predict skyrmion annihilation due to the inherent limitation that a continuum theory entails such as no possibility to nucleate Bloch lines, currently employed experimental techniques lack the combined time and space resolution required to analyze changes in the magnetization topology

with atomistic accuracy. So far the main focus has been on reproducible spin-orbit torque dynamics such as the displacement of skyrmions rather than on their annihilation [9,15,27,46–48]. For this reason the research presented in this paper constitutes a pioneer study on skyrmion annihilation induced by spin-orbit torques. Finally, we analyze how we can reliably annihilate the skyrmions by tailoring the pulse shape, which thus presents a quick and robust way to delete selected skyrmions.

II. METHOD AND RESULTS

The simulations were performed in a ferromagnetic disk with the radius of 53 nm and thickness of 3 nm, using the saturation magnetization $M_s = 10^6$ A/m, out-of-plane anisotropy constant $K_z = 1.3 \times 10^6$ J/m^3, the exchange constant $A = 1.1 \times 10^{-11}$ J/m, and the damping constant $\alpha = 0.5$. These parameters are comparable to those of CoFeB [49] in multilayer stacks that are widely used in thin film nanostructures [9]. In such systems skyrmions are stabilized by the Dzyaloshinskii-Moriya and magnetostatic interactions for a wide range of applied fields. The central part of the system was simulated atomistically (fine scale region), while the remaining part was simulated using the micromagnetic model (coarse scale region), following the approach described in Ref. [31]. The size of the fine scale region was chosen to fit the entire skyrmion at rest but without sacrificing too much computational time. The position of the fine scale region is automatically adjusted in order to contain the skyrmion spin structure. It should be stressed that larger skyrmions can still be simulated accurately as far as no discontinuities occur in the coarse scale region. First, magnetic Néel skyrmion states were relaxed for different values of the Dzyaloshinskii-Moriya interaction (DMI), then simulations with a constant uniform magnetic field applied in the direction opposite to the magnetization inside the skyrmion were performed. All the micromagnetic parameters were kept fixed, whereas the atomistic ones were changed. In particular, the distance a between two neighboring nodes of the mesh was changed, in order to increase the density of spins. While a can be interpreted as the lattice constant of the material, it is treated in this case just as a computational parameter. As a result, the magnetic moment of the spins μ and the exchange constant J were rescaled according to $\mu = a^3 M_s$ and $J = aA$. This effectively simulates materials that are consistent with the same micromagnetic parameters, which are used for the coarse scale region.

In Fig. 1(a) we show that an application of an external out-of-plane magnetic field leads to the skyrmion shrinking until it reaches its new equilibrium size. This behavior is reproduced for magnetic fields up to a critical value $H_{\rm del}$. For fields larger than $H_{\rm del}$, the skyrmion shrinks until it completely annihilates. The analysis of the skyrmion dynamics in nonzero out-of-plane fields shows that the spins magnetized in plane, corresponding to the center of the skyrmion's circular domain wall, tilt counter-clockwise while the skyrmion shrinks [see Figs. 1(b) and 2(b)]. When the shrinking stops, i.e., the skyrmion reaches a new equilibrium size, the magnetization in the domain wall aligns along the radial direction again, recovering the Néel skyrmion character.

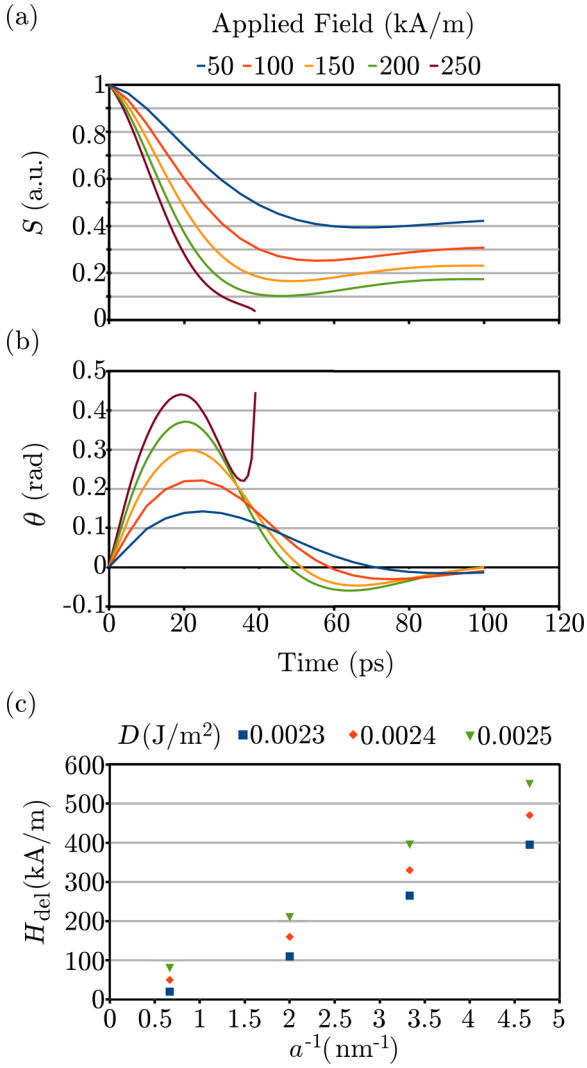

FIG. 1. Dynamics of a skyrmion for different values of a constant out-of-plane field. The system shows an oscillatory behavior, where both (a) its size, expressed in terms of the skyrmion magnetic moment S, and (b) the angle θ between the in-plane magnetization components of the domain wall and the radial direction, reach a certain nonzero value before relaxing back to the equilibrium. The data corresponding to 250 kA/m shows the skyrmion annihilation. (c) The minimum magnetic field $H_{\rm del}$ necessary to adiabatically annihilate a skyrmion for different values of the DMI constant D and linear spin density a^{-1}. $H_{\rm del}$ is shown to linearly increase as a function of the spin density. Data points corresponding to the lowest value of a^{-1} were simulated in purely micromagnetic simulations.

As a measure of the skyrmion size we use the total magnetic moment S inside the skyrmion's domain wall. It is proportional to $\sum_i (m_{z,i} - 1)$, where $m_{z,i}$ is the out-of-plane component of the normalized magnetization at the lattice site i, and the sum runs over all sites in the fine scale region, which always completely includes the skyrmion's domain wall. This allows one to evaluate the size of the skyrmion regardless of its shape. For fields below $H_{\rm del}$, we observe that S reaches a minimum, depending on the Gilbert damping α, before relaxing back to a slightly larger value [Fig. 1(a)]. While the skyrmion increases in size, the magnetization in the domain wall tilts

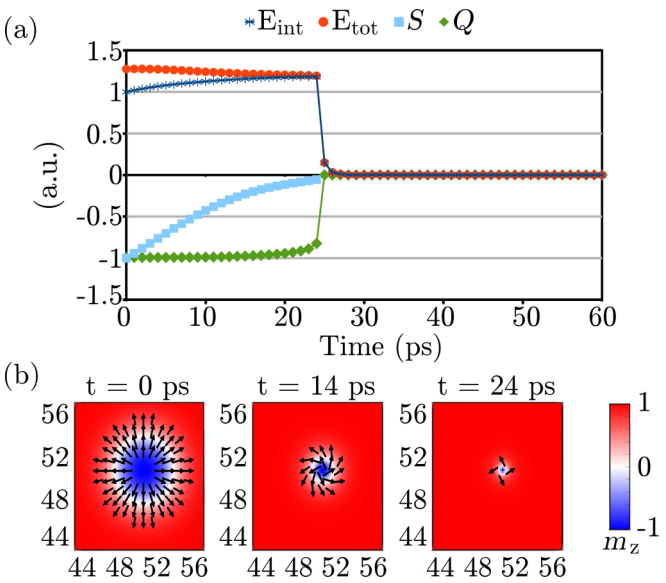

FIG. 2. (a) Path to annihilation of a skyrmion in 300 kA/m external magnetic field. The internal energy E_{int} of the system and the total energy (internal plus Zeeman energies) are compared as functions of time. A potential barrier exists for the internal energy which has to be overcome by the application of an external field. All the quantities are presented in arbitrary units. (b) Dynamic snapshots at various stages of the annihilation process. The initial configuration of a Néel skyrmion is perturbed when the structure is shrinking. The scale on the axes is expressed in units of the micromagnetic computational cell (3 nm).

counterclockwise [Fig. 1(b)]. The aim here is to demonstrate how the simulation results can be influenced by the refinement of the mesh rather than testing the stability of the skyrmion for different material parameters, as previously investigated, e.g., in Ref. [18].

We find that decreasing a, i.e., increasing the density of magnetic moments, leads to an increase of H_{del} [see Fig. 1(c)]. This is in agreement with Ref. [50] and shows how the minimum size which a skyrmion can reach before the annihilation strongly depends on the lattice constant.

The energy barrier [51–53] is shown in Fig. 2(a), where the internal energy E_{int} of a skyrmion shrinking under the influence of a constant magnetic field is plotted as a function of time. It can be noticed that E_{int}, consisting of the exchange, anisotropy, dipolar energy, and DMI contribution, increases until the annihilation occurs. The energy barrier is overcome by the application of the Zeeman energy. The skyrmion moment S is also shown, to stress that once the skyrmion reaches its minimum size, the topological barrier is overcome, and the system relaxes in the more stable uniform ferromagnetic state. It can be further noticed that the skyrmion charge Q instantly switches to zero when the barrier is overcome.

A purely micromagnetic simulation with a 1.5 nm cell size ($a^{-1} \simeq 0.667$ nm^{-1}) was included for comparison. It is paramount to stress that a multiscale approach is able to simulate the singularities atomistically using realistic material parameters, and the uniformly magnetized external region in the micromagnetic model. This allows one to predict the dynamics of a similar system with better quantitative accuracy than obtainable using only the micromagnetic model, making multiscale approaches the only existing method to realistically predict skyrmion annihilation.

Unlike the atomistic model, where the correct lattice constant must be used in order to obtain realistic results, the micromagnetic model becomes more and more accurate by refining the mesh. Ideally, in the infinitely fine mesh limit the analytical theory is recovered. Nevertheless even in the analytical theory, predictions made by the micromagnetic model can be in disagreement with the experimental evidence. These intrinsic limitations are derived from the micromagnetic model neglecting the length scales comparable to the lattice constant. The magnetization vector itself, which is the fundamental quantity that the model investigates, is proportional to the local average of the atomic magnetic moments. According to the definition [54]

$$\mathbf{M} = \lim_{\tau\to 0} \frac{1}{\tau} \sum_{i}^{N} \mu_i = \lim_{\tau\to 0} \frac{N}{\tau} \langle \mu \rangle, \tag{2}$$

where τ indicates a volume element containing N magnetic moments μ. The limit $\tau \to 0$ should be considered to be restricted to the volume of elements which are small compared to the full magnetic system but large enough to contain a statistically significant number of magnetic moments. Basic examples are Bloch points [55,56] and the excitation of spin waves with a wavelength smaller than the lattice constant, a phenomenon that does indeed arise in a continuum model despite being forbidden in experiments and in realistic atomistic simulations. This thus shows that the micromagnetic model cannot be applied to systems where changes in the magnetization occur on a length scale comparable to the atomic lattice.

As the annihilation of a skyrmion includes the formation and the annihilation of a BL, this phenomenon cannot be properly simulated in the micromagnetic framework. Because of this change in topology of the spin structure during the process [24], the charge Q of the structure changes from ± 1 to 0, thus lifting the topological protection. While previously field induced dynamics was studied, and in Ref. [21] a BL is formed and annihilated in a Bloch skyrmion via application of a field gradient, here we study a singularity generated by a spin-polarized current pulse applied along the x direction. In general, using spin currents is more advantageous than using fields to manipulate magnetization due to more favorable scaling. The influence of the spin-orbit torques on skyrmions [45] in particular yields many promising possibilities towards the implementation of skyrmions as information bits. The LLG equation implemented to include the effect of a spin-polarized current (generated for instance via the inverse spin galvanic effect or the spin-Hall effect) [44] reads:

$$\begin{aligned}\frac{d\mathbf{m}}{dt} = &-\gamma'[\mathbf{m}\times\mathbf{H}_{\text{eff}} + \alpha(\mathbf{m}\times(\mathbf{m}\times\mathbf{H}_{\text{eff}}))] \\ &-\gamma' a_J[(\xi-\alpha)(\mathbf{m}\times\mathbf{p}) + (1+\alpha\xi)(\mathbf{m}\times(\mathbf{m}\times\mathbf{p}))],\end{aligned} \tag{3}$$

where $\gamma' = \gamma/(1+\alpha^2)$ with γ being the gyromagnetic ratio, $\mathbf{H}_{\text{eff}}$ is the effective field, $\mathbf{p}$ the average polarization of the current generated by the spin-Hall effect, $a_J = \hbar/2(\alpha_H \times J)/(2eM_s d\mu_0)$ (where α_H is the Hall angle, d the thickness

of the system, J the current density), the dampinglike term [57–59], and ξ the ratio between dampinglike and fieldlike torques. We apply current density pulses of Gaussian shape, $J(t) = J_0 \exp[-t^2/(2\sigma^2)]$.

We find that the annihilation of BLs can be excited in a Néel skyrmion for some combinations of J_0 and σ. The material parameters employed for this simulation were the same as the stability simulations with the damping constant $\alpha = 0.1$. Furthermore the Hall angle $\alpha_H = 0.1$ and the constant $\xi = 0.5$ were used.

The results show that it is indeed possible to form a vertical BL, as a vortex-antivortex couple on the domain wall of the skyrmion, using spin-orbit torques. In the process the domain wall deforms, increases in width on one side of the skyrmion, and decreases on the opposite side. The duration of the pulse plays a fundamental role, since a pulse that is too short would not deform the domain wall of the Skyrmion enough, while a pulse too long would act adiabatically on the whole skyrmion and push it beyond the edge of the magnetic system. Intermediate values result in the formation of the BL

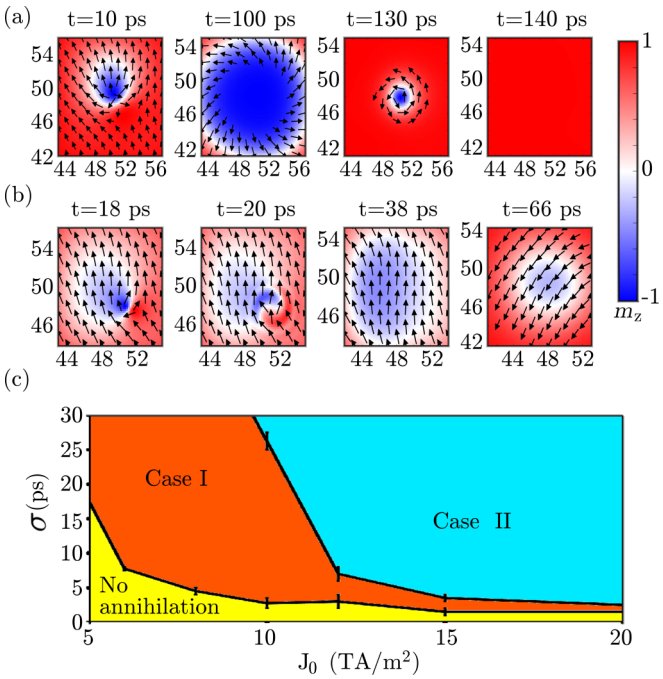

FIG. 3. Spin structure of the skyrmion during the annihilation process in cases I and II. The color code shows the out-of-plane component, from red, to white, to blue. The initial state corresponds to a relaxed skyrmion centered on the cell with coordinates (50, 50). (a) Case I: A BL is formed in the domain wall of the skyrmion within a vortex-antivortex pair. The spins in the domain wall turn counter-clockwise starting from the position of the pair, meanwhile, the skyrmion increases in size and reaches a maximum then starts shrinking in size. As the skyrmion shrinks below the minimum size, it is finally annihilated. The system relaxes into the ferromagnetic ground state. (b) Case II: The vortex-antivortex pair annihilates, the skyrmion number immediately turns to zero, the system quickly relaxes back to the ferromagnetic state. (c) Different regimes depending on the peak height J_0 and half-width σ of the Gaussian pulse. The error bars were evaluated by performing simulations with different values of σ.

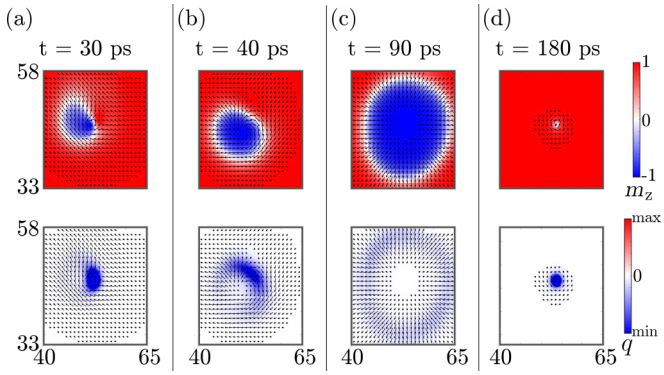

FIG. 4. Details of the case I annihilation process. (a) The topological charge density is accumulated in a vortex-antivortex pair. (b) The system relaxes. (c) The skyrmion size increases until the Néel character is recovered. (d) The skyrmion shrinks and then annihilates. For the topological charge density q the relation min $= -$max holds.

that can either annihilate or relax. While the annihilation is a topological transformation and leads to the annihilation of the skyrmion, the relaxation of the BL results in its rapid expansion. We can explain the rapid expansion of the skyrmion as a consequence of the large exchange energy density of the BL being dissipated in the breathing mode excitation of the skyrmion. It is possible to distinguish three different regimes, see Fig. 3. In the nonannihilating regime the relaxation of the BL is accompanied by size oscillations of the skyrmion, which do not lead to collapse. As was noted earlier in the paper, skyrmions collapse once their size becomes too small to stabilize them in the antiparallelly aligned surrounding magnetization. This occurs in the annihilation regime of case I [Fig. 4], which (while qualitatively similar to the nonannihilating regime) results in stronger size oscillations that annihilate the skyrmion due to overshooting in the shrinking phase. The annihilation regime of case II, see Fig. 5, is indeed qualitatively different since the vortex-antivortex pair with opposite polarities forms and subsequently annihilates [51,60], leading to the immediate annihilation of the skyrmion. This regime could thus be exploited for practical applications since

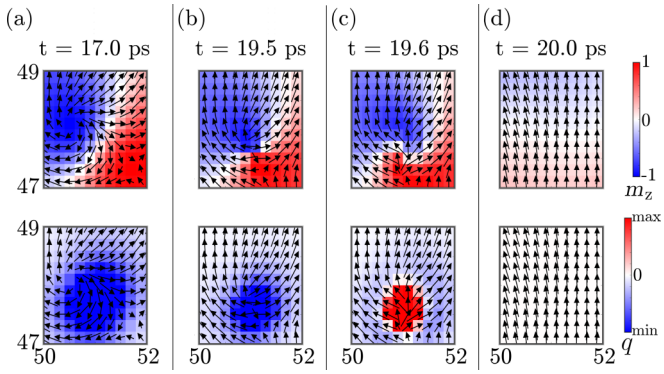

FIG. 5. Zoom in on the case II annihilation process. (a) The topological charge density is contained in a vortex-antivortex pair. (b) A Bloch line is formed. (c) The Bloch line annihilates, generating a topological charge density of the opposite sign. (d) The system relaxes into the ferromagnetic state. For the topological charge density q the relation min $= -$max holds.

it allows one to lift the topological protection of skyrmions in a quick and reliable manner.

In both annihilation cases, a spike occurs in the topological charge density q. In case II, the structure corresponding to the spike in q is a very tight Bloch line separating a vortex core from an antivortex core. In this phase, the interplay between the energy contributions provided by the exchange interaction and the DMI plays a crucial role. At the moment of annihilation a topological charge of the opposite sign is generated within the peak in q. This corresponds to neighboring spins tilting in the direction opposite to the one favored by the sign of the DMI. This provides an increase in the DMI energy that is balanced by the decreasing exchange energy. The system then relaxes to a uniformly magnetized state. While the two opposite topological charges annihilate each other, both the energy contributions decrease, reaching a lower minimum of the total energy. The movies showing the two processes in detail are included as Supplemental Material [61].

III. CONCLUSIONS

In conclusion, we have determined the skyrmion stability using a multiscale approach that allows for a more realistic description of skyrmion annihilation compared to conventionally used micromagnetics. We have demonstrated that the stability of skyrmions is strongly influenced by computational parameters, such as the mesh size. Using the multiscale approach overcomes this problem and allows one to obtain the realistic skyrmion stability parameters. The cell size here is fixed by the appropriate lattice constant of the simulated material, and the computational efforts are far lower than those of a purely atomistic simulation. Furthermore, this approach reproduces the dynamics including the spin spectrum realistically, which even allows in the future to include thermal effects. We employ this multiscale approach to study topological transformations by applying spin-orbit torques due to spin-polarized current pulses, introducing the possibility to annihilate skyrmions by applying a properly tailored pulse. This is shown to be a very fast and efficient method to delete isolated skyrmions as required for applications. We ascertain the combinations of pulse parameters, which robustly annihilate the skyrmion. This may open up a path to delete skyrmions reliably as required for future spintronic memory.

ACKNOWLEDGMENTS

A.D.L. and K.L. are recipients of a scholarship through the Excellence Initiative by the Graduate School Materials Science in Mainz (GSC 266); B.K. is the recipient of a Carl Zeiss Postdoc Scholarship - Multiskalensimulationen für energiesparende Magnetisierungsmanipulation. The authors acknowledge the support of SpinNet (DAAD Spintronics network, Project No. 56268455), MaHoJeRo (DAAD Spintronics network, Project No. 57334897), and the DFG (SFB TRR 173 SPIN+X). M.K. thanks ICC-IMR at Tohoku University for their hospitality during a visiting researcher stay at the Institute for Materials Research. O.A.T. acknowledges support by the Grants-in-Aid for Scientific Research (Grants No. 25247056, No. 15H01009, No. 17K05511, and No. 17H05173) from MEXT, Japan. O.A.T. was supported in part by JSPS and RFBR under the Japan - Russia Research Cooperative Program.

[1] T. H. R. Skyrme, Nucl. Phys. **31**, 556 (1962).
[2] X. Z. Yu, Y. Onose, N. Kanazawa, J. H. Park, J. H. Han, Y. Matsui, N. Nagaosa, and Y. Tokura, Nature (London) **465**, 901 (2010).
[3] S. Seki, X. Z. Yu, S. Ishiwata, and Y. Tokura, Science **336**, 198 (2012).
[4] M. Bode, M. Heide, K. von Bergmann, P. Ferriani, S. Heinze, G. Bihlmayer, A. Kubetzka, O. Pietzsch, S. Blügel, R. Wiesendanger, Nature (London) **447**, 190 (2007).
[5] S. Heinze, K. von Bergmann, M. Menzel, J. Brede, A. Kubetzka, R. Wiesendanger, G. Bihlmayer, and S. Blügel, Nat. Phys. **7**, 713 (2011).
[6] A. Bogdanov and A. Hubert, J. Magn. Magn. Mater. **138**, 255 (1994).
[7] U. K. Rößler, A. N. Bogdanov, C. Pfleiderer, Nature (London) **442**, 797 (2006).
[8] S. Mühlbauer, B. Binz, F. Jonietz, C. Pfleiderer, A. Rosch, A. Neubauer, R. Georgii, and P. Böni, Science **323**, 915 (2009).
[9] S. Woo, K. Litzius, B. Krüger, M.-Y. Im, L. Caretta, K. Richter, M. Mann, A. Krone, R. M. Reeve, M. Weigand, P. Agrawal, I. Lemesh, M.-A. Mawass, P. Fischer, M. Kläui, and G. S. D. Beach, Nat. Mater. **15**, 501 (2016).
[10] S. Rohart and A. Thiaville, Phys. Rev. B **88**, 184422 (2013).
[11] M. Beg, R. Carey, W. Wang, D. Cortés-Ortuño, M. Vousden, M.-A. Bisotti, M. Albert, D. Chernyshenko, O. Hovorka, R. L. Stamps, and H. Fangohr, Sci. Rep. **5**, 17137 (2015).
[12] A. Fert, J. Sampaio, and V. Cros, Nat. Nanotech. **8**, 152 (2013).
[13] J. Sampaio, V. Cros, S. Rohart, A. Thiaville, and A. Fert, Nat. Nanotech. **8**, 839 (2013).
[14] G. Finocchio, F. Büttner, R. Tomasello, M. Carpentieri, and M. Kläui, J. Phys. D: Appl. Phys. **49**, 423001 (2016).
[15] K. Litzius, I. Lemesh, B. Krüger, P. Bassirian, L. Caretta, K. Richter, F. Büttner, K. Sato, O. A. Tretiakov, J. Förster, R. M. Reeve, M. Weigand, I. Bykova, H. Stoll, G. Schütz, G. S. D. Beach, and M. Kläui, Nat. Phys. **13**, 170 (2017).
[16] S. Krause and R. Wiesendanger, Nat. Mater. **15**, 493 (2016).
[17] N. Romming, C. Hanneken, M. Menzel, J. E. Bickel, B. Wolter, K. von Bergmann, A. Kubetzka, and R. Wiesendanger, Science **341**, 636 (2013).
[18] L. Cai, E. M. Chudnovsky, and D. A. Garanin, Phys. Rev. B **86**, 024429 (2012).
[19] D. Cortés-Ortuño, W. Wang, M. Beg, R. A. Pepper, M.-A. Bisotti, R. Carey, M. Vousden, T. Kluyver, O. Hovorka, and H. Fangohr, Sci. Rep. **7**, 4060 (2017).
[20] I. S. Lobanov, H. Jónsson, and V. M. Uzdin, Phys. Rev. B **94**, 174418 (2016).

[21] C. Moutafis, S. Komineas, and J. A. C. Bland, Phys. Rev. B **79**, 224429 (2009).
[22] J. C. Slonczewski, J. Appl. Phys. **45**, 2705 (1974).
[23] S. Iwatsuka and S. Iida, Jpn. J. Appl. Phys. **22**, 1855 (1983).
[24] V. G. Bar'yakhtar, E. B. Krotenko, and D. A. Yablonskii, Zh. Eksp. Teor. Fiz **91**, 921 (1986) [Sov. Phys. JETP **64**, 542 (1986)].
[25] K. Matsuyama, K. Chikamatsu, and H. Asada, IEEE Trans. Magn. **26**, 2517 (1990).
[26] L. Arnaud, B. J. Youssef, D. Challeton, and J. Miltat, Bloch line magnetic memory, US Patent 5260891 A (1990).
[27] W. Jiang, P. Upadhyaya, W. Zhang, G. Yu, M. B. Jungfleisch, F. Y. Fradin, J. E. Pearson, Y. Tserkovnyak, K. L. Wang, O. Heinonen, S. G. E. te Velthuis, and A. Hoffmann, Science **349**, 283 (2015).
[28] D. A. Gilbert, B. B. Maranville, A. L. Balk, B. J. Kirby, P. Fischer, D. T. Pierce, J. Unguris, J. A. Borchers, and K. Liu, Nat. Commun. **6**, 8462 (2015).
[29] J. Barker and O. A. Tretiakov, Phys. Rev. Lett. **116**, 147203 (2016).
[30] A. Thiaville, J. M. García, R. Dittrich, J. Miltat, and T. Schrefl, Phys. Rev. B **67**, 094410 (2003).
[31] A. De Lucia, B. Kruger, O. A. Tretiakov, and M. Kläui, Phys. Rev. B **94**, 184415 (2016).
[32] C. J. Garcìa-Cervera and A. M. Roma, IEEE Trans. Magn. **42**, 1648 (2006).
[33] K. M. Tako, T. Schrefl, M. A. Wongsam, and R. W. Chantrell, J. Appl. Phys. **81**, 4082 (1997).
[34] F. Garcia-Sanchez, O. Chubykalo-Fesenko, O. Mryasov, R. W. Chantrell, and K. Y. Guslienko, Appl. Phys. Lett. **87**, 122501 (2005).
[35] F. Garcia-Sanchez, O. Chubykalo-Fesenko, O. Mryasov, and R. W. Chantrell, Physica B (Amsterdam) **372**, 328 (2006).
[36] F. Garcia-Sanchez, O. Chubykalo-Fesenko, O. Mryasov, R. W. Chantrell, and K. Y. Guslienko, J. Appl. Phys. **97**, 10J101 (2005).
[37] T. Jourdan, A. Marty, and F. Lancon, Phys. Rev. B **77**, 224428 (2008).
[38] T. Jourdan, A. Masseboeuf, A. Marty, F. Lancon, and P. Bayle-Guillemaud, J. Appl. Phys. **106**, 073913 (2009).
[39] C. Andreas, A. Kakay, and R. Hertel, Phys. Rev. B **89**, 134403 (2014).
[40] F. Bruckner, M. Feischl, T. Führer, P. Goldenits, M. Page, D. Praetorius, M. Ruggeri, and D. Suess, Math. Models Methods Appl. Sci. **24**, 2627 (2014).
[41] P. Weinberger, E. Y. Vedmedenko, R. Wieser, and R. Wiesendanger, Philos. Mag. **91**, 2248 (2011).
[42] See Supplemental Material at http://link.aps.org/supplemental/10.1103/PhysRevB.96.020405 for further explanations of the multiscale approach and analysis used.
[43] A. Brataas and K. M. D. Hals, Nat. Nanotech. **9**, 86 (2014).
[44] M. Hayashi, J. Kim, M. Yamanouchi, and H. Ohno, Phys. Rev. B **89**, 144425 (2014).
[45] I. A. Ado, O. A. Tretiakov, and M. Titov, Phys. Rev. B **95**, 094401 (2017).
[46] Y. Liu, G. Yin, J. Zang, J. Shi, and R. K. Lake, Appl. Phys. Lett. **107**, 152411 (2015).
[47] X. Z. Yu, N. Kanazawa, W. Z. Zhang, T. Nagai, T. Hara, K. Kimoto, Y. Matsui, Y. Onose, and Y. Tokura, Nat. Commun. **3**, 988 (2012).
[48] O. Boulle, J. Vogel, H. Yang, S. Pizzini, D. de Souza Chaves, A. Locatelli, T. O. Menteş, A. Sala, L. D. Buda-Prejbeanu, O. Klein, M. Belmeguenai, Y. Roussigné, A. Stashkevich, S. M. Chérif, L. Aballe, M. Foerster, M. Chshiev, S. Auffret, I. M. Miron, and G. Gaudin, Nat. Nanotechnol. **11**, 449 (2016).
[49] X. Liu, W. Zhang, M. J. Carter, and G. Xiao, J. Appl. Phys. **110**, 033910 (2011).
[50] A. Siemens, Y. Zhang, J. Hagemeister, E. Y. Vedmedenko, and R. Wiesendanger, New J. Phys. **18**, 045021 (2016).
[51] O. A. Tretiakov and O. Tchernyshyov, Phys. Rev. B **75**, 012408 (2007).
[52] F. Büttner, I. Lemesh, and G. S. D. Beach, arXiv:1704.08489.
[53] G. Yin, Y. Li, L. Kong, R. K. Lake, C. L. Chien, and J. Zang, Phys. Rev. B **93**, 174403 (2016).
[54] C. Mencuccini and V. Silvestrini, *Fisica 2. Elettromagnetismo-ottica.* (Liguori, Napoli, 1998).
[55] W. Döring, J. Appl. Phys. **39**, 1006 (1968).
[56] O. V. Pylypovskyi, D. D. Sheka, and Y. Gaididei, Phys. Rev. B **85**, 224401 (2012).
[57] J. C. Slonczewski, J. Magn. Magn. Mater. **159**, L1 (1996).
[58] L. Berger, Phys. Rev. B **54**, 9353 (1996).
[59] S. Zhang, P. M. Levy, and A. Fert, Phys. Rev. Lett. **88**, 236601 (2002).
[60] R. Hertel and C. M. Schneider, Phys. Rev. Lett. **97**, 177202 (2006).
[61] See Supplemental Material at http://link.aps.org/supplemental/10.1103/PhysRevB.96.020405 for the videos of the skyrmion annihilation.